Contents list available at CBIORE journal website

International Journal of Renewable Energy Development

Journal homepage: https://ijred.cbiore.id

Research Article

Evaluating the performance of stainless steel in microbial electrolysis cells: Hydrogen production and corrosion behaviour

Raba'atun Adawiyah Shamsuddin[a], Mimi Hani Abu Bakar[b*], Wan Ramli Wan Daud[c], Kim Byung Hong[d,e], Jamaliah Md. Jahim[c], Wan Syaidatul Aqma Wan Mohd Noor[f], Rozan Mohamad Yunus[b], Ibdal Satar[g], Fabrice Ndayisenga[h]

[a]*Institute of Sustainable Energy & Resources, Universiti Teknologi PETRONAS, Bandar Seri Iskandar, 32610 , Malaysia*

[b]*Fuel Cell Institute, The National University of Malaysia, 43600 UKM Bangi, Malaysia*

[c]*Department of Chemical and Process Engineering, Faculty of Engineering and Built Environment, The National University of Malaysia, 43600 UKM Bangi, Malaysia*

[d]*Korea Institute of Science and Technology, Seoul 136-791, Korea*

[e]*State Key Laboratory of Urban Water Resource and Environment, Harbin Institute of Technology, Harbin 150090, China*

[f]*Department of Biological Sciences & Biotechnology, Faculty of Science & Technology, The National University of Malaysia, 43600 UKM Bangi, Malaysia*

[g]*Food Technology Development, Faculty of Industrial Technology Universitas Ahmad Dahlan Bantul 55191 Yogyakarta Indonesia*

[h]*College of Resources and Environment, University of Chinese Academy of Sciences, 19 A Yuquan Road, Beijing 100049, P.R. China*

Abstract. Microbial Electrolysis Cells (MECs) provide a sustainable route to hydrogen production via microbial electron transfer, while the biocathode enhances affordability and functionality. Stainless steel (SS) is an ideal material for bioelectrochemical systems (BES) due to its high recyclability and corrosion resistance. The chromium content forms a protective, corrosion-resistant layer that promotes beneficial microbial interactions and enhances durability. However, the MEC requires an oxygen-free cathode, which is incompatible with the layer. This study evaluated the corrosion resistance of SS to microbial interactions, also known as microbial-influenced corrosion (MIC). The results from SS are compared with those from carbon steel (CS) and graphite felt (GF), which are standard laboratory electrode materials used as controls. The performance of these biocathodes was assessed in both open-circuit (Co-MEC) and closed-circuit (Cc-MEC) conditions over a 120-day operational period, with a focus on hydrogen production and corrosion resistance against MIC. SS biocathodes exhibited the highest hydrogen production rate (2.33 ± 0.34 LH_2/m^2. day), outperforming CS by 54% and GF by 1.3%. Additionally, the SS system demonstrated superior chemical oxygen demand (COD) removal efficiency, achieving 45% COD removal, comparable to the GF (44%), whereas CS achieved 38%. The corrosion analysis revealed that the corrosion rate (RM) of CS (0.08 ± 0.08 mm/year) was 86% higher than that of SS and GF (0.03 ± 0.03 mm/year) under Cc-MEC mode. Microbial community analysis revealed a higher abundance of *Desulfovibrio,* a genus within the sulphate-reducing bacteria (SRB) group, in Co-MEC systems, which contributes to increased corrosion. In contrast, the Cc-MEC system showed an increase in electrochemically active bacteria (EAB), including *Pseudomonas*, which are known to promote hydrogen evolution and inhibit SRB. This study highlights the need for further research into corrosion-resistant materials and the optimisation of microbial communities.

Keywords: Stainless steel, MEC biocathode, Microbiologically-influenced corrosion, Pitting, SRB, Fuel Cell, Application, SDG 7

Received: 1st July 2025; Revised: 16th Nov 2025; Accepted: 26th Dec 2025; Available online: 11th January 2026

1. Introduction

The growth of industry and population has increased global energy demand (Yu *et al.*, 2022). To date, we still heavily depend on non-renewable fossil fuels as our primary energy source (Tahir *et al.*, 2022). However, the world is now compelled to seek alternative energy sources due to increasing demand for renewable energy, environmental protection, and price fluctuations driven by supply-demand imbalances, geopolitical events, and market speculation (Dutt, 2022). Due to its adaptability and ability to provide energy to isolated communities, hydrogen has become a popular alternative fuel. Governments and the private sector have invested substantial capital in research, development, and infrastructure to build hydrogen manufacturing plants, distribution networks, and fuel cells. Furthermore, the growing global population increase environmental pollution, including waste generation. In this regard, bioelectrochemical systems (BESs) have been reviewed, in which the systems can adopt microbes as catalysts to consume waste, while generating green, clean energy, which in turn reduces the chemical oxygen demand (COD) from the pollution (Cabrera & Agudelo-Escobar, 2023; Maureira *et al.*, 2023).

* Corresponding author
Email: mimihani@ukm.edu.my (M.H.Abu Bakar)

https://doi.org/10.61435/ijred.2026.61531
ISSN: 2252-4940/© 2026.The Author(s). Published by CBIORE

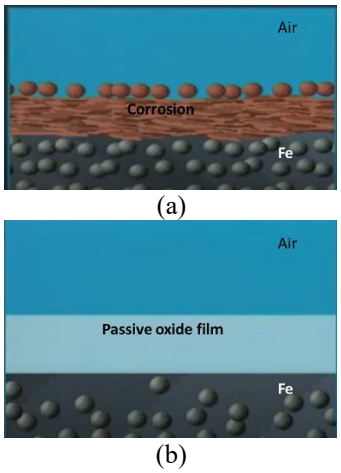

Fig. 1 (a) Corrosion occurs on a standard iron bar (Fe), and (b) a passive oxide film (light blue layer on the surface) protects Fe from exposure to oxygen.

Among the family of BESs, a microbial electrolysis cell (MEC) is capable of performing the hydrogen evolution reaction (HER) through microbially released electrons (Bora *et al*., 2022; Guerrero-Sodric *et al*., 2024), while reducing the contamination that fuels it. Platinum (Pt) has traditionally been used as a catalyst for HER in MEC cathodes due to its high catalytic activity, which accelerates hydrogen production, provides low overpotentials, and offers notable stability. However, the high cost carried by the Pt has encouraged researchers to explore cheaper and greener alternatives (Bora *et al*., 2022; Shamsuddin *et al*., 2019). Electrochemically active bacteria (EAB) have emerged as a promising alternative catalyst solution at the cathode, offering affordability since they can be sourced from the wastewater stream, perform self-regeneration, and are a readily available resource (Shaikh *et al*., 2021; Shi *et al*., 2024). Croese *et al.* demonstrated the effectiveness of graphite felt (GF) as biocathodes in MECs for achieving significant hydrogen production rates of 630 LH_2/ m^3.day (Croese *et al*., 2011). They have added the *Geobacter sulfurreducens,* which are EAB and well known for hydrogen production in MEC to assist the plain GF electrodes. The EAB, alongside conductive materials like GF or common metals like stainless steel (SS) and carbon steel (CS), forms a biocathode and drives the desired cathode reaction (Bora *et al*., 2022; Croese *et al*., 2011; Ewing *et al*., 2017). The cathode accepts electrons from the anode. It also provides a surface for microorganisms to attach to and catalyses the reaction of electrons and protons in the electrolyte to form hydrogen gas. Thus, factors such as electrical conductivity, mechanical strength, and corrosion resistance are crucial in selecting bioelectrode materials for any BES, including MEC.

The SS has been utilised as the anode in a microbial fuel cell (MFC) setting, which can be considered the simplest form of BES. The metal offers a reduction in the MFC polarisation resistance, which refers to the ease with which electrons are passed from the microbe to the electrode (Hemdan *et al*., 2023) compared to carbon-based electrodes.

In addition, the SS possesses superior tensile strength and durability and is more recyclable than GF. Importantly for bioelectrochemical applications, SS also demonstrates an affinity for EAB biofilm formation (Long *et al*., 2024). SS is an alloy made primarily from iron with at least 10.5% chromium alloy and other metals, such as nickel, manganese, molybdenum, copper, and other elements of carbon, nitrogen, sulphur and silicon. Adding other elements, such as chromium, to the iron helps increase resistance to corrosion (**Fig. 1**(a)) and extreme temperatures, improving strength, weldability, formability, and controlling magnetism (Bunsen, 2010). When in an oxygen environment, chromium in the SS produces a stable, chromium-rich oxide, also known as a passive oxide film, on exposed surfaces, protecting the underlying metal from oxidising (corroding) (Singh *et al*., 2022) (**Fig. 1**(b)). However, in contrast, the MEC requires the cathode to be oxygen-free while donating electrons.

The MEC cathode is in an anaerobic state, retaining wastewater rich in electron acceptors, such as microorganisms, sulphates, and aggressive ions. Under a non-MEC system that is oxygen-free, these factors can facilitate SS corrosion through certain anaerobic bacteria, which is also known as microbially influenced corrosion (MIC) (Lou *et al*., 2021; Song *et al*., 2023; J. Zhao *et al*., 2010). MIC, driven by soil microbes and acid-producing bacteria like *Clostridium*, poses a severe threat to industries including chemical processing, marine, oil, and gas (Moura *et al*., 2018), leading to pitting corrosion on steels and causing material deterioration and significant economic losses (Telegdi *et al*., 2017). The involvement of the MIC towards electrode materials through extracellular electron transfer (EET) processes has been examined (B. H. Kim *et al*., 2015; Rosenbaum *et al*., 2011; Shamsuddin *et al*., 2019). Some studies suggest microbial EET may induce corrosion by directly absorbing electrons from metallic iron (Kato, 2016; Lou *et al*., 2021; Song *et al*., 2023). In addition, an electron mediator such as sulfate could also worsen MIC (Lou *et al*., 2021; E. Zhou *et al*., 2022). Bacteria under the sulphate-reducing bacteria (SRB) group are primarily responsible for nickel (Ni), CS, and SS corrosion under anaerobic conditions (Kato, 2016; Song *et al*., 2023; E. Zhou *et al*., 2022). Concurrently, *Desulfovibrio* bacteria, also from the SRB, a member of the Proteobacteria phylum, are capable of hydrogen production with the help of the hydrogenase enzyme and consumption (Guerrero-Sodric *et al*., 2024; Wu *et al*., 2022) as follows:

Hydrogen production:

$$CH_3COO^- + 4H_2O \rightarrow 2HCO_3^- + 9H^+ + 8e^- \quad \text{(Eq. 1)}$$

$$2H^+ + 2e^- \rightarrow H_2 \text{ (involve hydrogenase enzyme)} \quad \text{(Eq. 2)}$$

Hydrogen consumption:

$$4H_2 + SO_4^{2-} + H^+ \rightarrow HS^- + 4H_2O \quad \text{(Eq. 3)}$$

The pathway to produce (Eq.1 and Eq.2) or consume (Eq.3) hydrogen will be based on the abundance of the organic acid or the sulphate (Bora *et al*., 2022; B. H. Kim *et al*., 2015; Lim *et al*., 2018). Consequently, these bacteria use metals as electron donors or energy sources (E. Zhou *et al*., 2022).

For a closed-circuit MEC, the bioanode and cathode electrode reaction resembles cathodic protection (CP). CP is a critical method for preventing corrosion on large metal surfaces that require protection, particularly cathodes (Khan *et al*., 2018; Wang *et al*., 2020). It is typically achieved using a sacrificial anode or an external power source that supplies electrons to the protected metal, thereby making the protected metal the cathode (Wang *et al*., 2020) and preventing corrosion. However, a significant question remains about the effectiveness of the CP method in protecting SS as an MEC cathode electrode from corrosion by MIC. The answer can address the practical viability of using material for cathodes in real-world MEC applications. This study examines three types of common electrode materials for MEC: SS, CS, and GF, when exposed to MIC environments under closed (Cc) and open-circuit (Co) conditions. The closed-circuit MEC system mimics CP by maintaining a continuous electron flow to the cathode, which may reduce MIC-induced

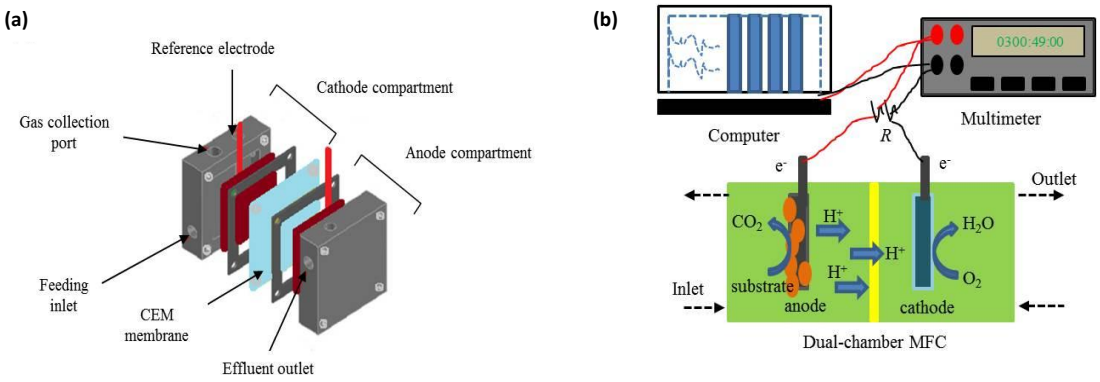

Fig. 2 Schematic diagram of the (a) MEC compartment and (b) operation of the dual-chamber MEC in this study.

corrosion on these materials. Each set of MEC biocathodes was built in replicate, followed by analyses of corrosion resistance, surface morphology, and a typical MEC analysis of hydrogen production. Finally, high-throughput sequencing of the V4 region of the 16S rRNA gene was used to identify the microbial communities responsible for cathode biofilm formation and to assess their contributions to corrosion and hydrogen production.

2. Materials and Methods

2.1 Dual-chamber MEC Set-up

Following four months of operation as anodes in MFCs with SS, CS, and GF materials, the biofilmed electrodes were repurposed as electrodes in dual-chamber closed-circuit MECs (Cc-MECs) (**Fig. 2**), designated as Cc-MEC-SS, Cc-MEC-CS, and Cc-MEC-GF. The electrodes underwent annealing before MFC application, as described in Shamsuddin *et al.*, to enhance biofilm attachment (Shamsuddin *et al.*, 2018). In this experiment, the inocula for the anode and cathode were obtained from a diverse microbial community in lake mud and filtered to remove large particles. The cathodic medium was filled with 0.41 g/L $NaHCO_3$, 0.1 g/L $(NH_4)_2SO_4$, 0.11 g/L KCl, 0.66 g/L NaH_2PO_4 . $2H_2O$, 1.03 g/L $Na_2HPO_4 \cdot 2H_2O$, 12.5 mL trace amount of Wolfe's mineral, and 5.0 mL vitamin solution. The medium was sterilised by autoclaving at 121 °C for at least 15 minutes. For the anodic compartment, 1.0 g/L CH_3COONa, 1.0 g/L yeast, 0.31 g/L NH_4Cl, 0.13 g/L KCl, 4.58 g/L Na_2HPO_4, 2.45 g/L NaH_2PO_4. H_2O, 12.5 mL trace amount of Wolfe's mineral and 5.0 mL vitamin solution, similar to those used in a previous study, were prepared (Shamsuddin *et al.*, 2018). The ratio of filtered inoculum to the respective compartment medium was 50:50 for both the anodic and cathodic inocula. After 120 days of operating as Cc-MEC, three sets of open-circuit MEC (Co-MEC) systems were derived from the available Cc-MEC reactors: Co-MEC-SS, Co-MEC-CS, and Co-MEC-GF.

2.2 Electrochemical Operation

In the Cc-MEC operation, SS, CS, and GF cathodes were connected to a 1 kΩ external resistance via titanium wires, whereas in the Co-MEC condition, all cathodes were disconnected. Both reactor sets were triplicated at room temperature (25 ± 1 °C) under anaerobic conditions. To ensure anaerobic conditions were maintained and to facilitate HER, each cathode chamber was purged with 99.99% hydrogen for 5 min. The GF cathode served as the control for monitoring corrosion behaviour throughout the experiment.

2.2.1 Current Density

In MEC operation, the output voltage was recorded using a multimeter data acquisition system (Model 2700, Keithley, USA) connected to a personal computer, and readings were taken every five minutes. The current density (I_v, A/m²) was calculated using Ohm's law, as described below (Eqs. 4 and 5).

$$I_v = I / A \quad \text{(Eq. 4)}$$

$$I = V / R \quad \text{(Eq. 5)}$$

Where I is the current measured (A), V is the voltage measured (V), R is the external load (Ω), and A is the geometric surface area of the anode (5 cm x 4 cm). An external resistance of 1 kΩ was employed, and a fixed power supply voltage of 1.1 V (Keithley 2230-30-1 multi-channel programmable DC PS) was used to provide the energy and catalyse the substrate into by-products at the cathode.

2.3 Corrosion Evaluation

The effects of corrosion on the metal were examined by operating the MEC reactors under closed-circuit and open-circuit conditions. Electrochemical corrosion tests were conducted during the fourth month of Cc- and Co-MEC operations using potentiodynamic polarisation (PDP) with a three-electrode configuration comprising a working electrode, a reference electrode, and a counter electrode. The PDP analysis was performed at a 1 mV/s scan rate, adapted from Mohd Rasid *et al*(Mohd Rasid *et al.*, 2017) and Zhou *et al.* (H. Zhou *et al.*, 2022), using an AUTOLAB potentiostat (PGSTAT128N, Utrecht, Netherlands). The PDP technique yields the slope from the Tafel plot, enabling estimation of the corrosion current density, which is subsequently converted to a corrosion rate (R_M). The PDP measurements were repeated three times, and the values were averaged.

2.3.1 Calculation of Corrosion Rates

Eq. 6 was used to calculate the R_M from the corrosion current, which depends on both anodic (oxidation) and cathodic (reduction) reactions.

$$R_M = [0.13 I_{corr}\,(\mathrm{EW})] / d \quad \text{(Eq. 6)}$$

Where I_{corr} is the corrosion current density normalised by the cathode electrode volume, which is the same as the anode (5 cm x 4 cm x 0.5 cm), EW is the equivalent weight of the metal sample (g), and d is the density of the metal (g/cm³).

2.4 Hydrogen Evolution Rate

The gas generated at the MEC cathode was collected in a glass tube using the water displacement method. Samples were obtained from the top of the glass tube through septa using a syringe. The gas composition was later analysed using offline gas chromatography (GC) (HP 4890D) equipped with a thermal conductivity detector and two packed columns (80/100 HayeSep and 80/100 Chromosorb 102 support). High-purity helium (99.99%) was used as the carrier gas for GC and set at 25 mL/min. The produced gases were identified by retention time, and the percentages of gases in the chromatogram were determined from peak areas. Based on the GC analysis data, the actual gas volume (V_g) was calculated as in Eq. 7.

$$V_g = (V_h)\,(X_g) \quad \text{(Eq 7)}$$

V_g (L) is the actual gas volume, V_h (L) is the amount of gas captured in the glass tube, and X_g is the volumetric gas fraction in the gas samples obtained from the GC analysis. The gas production rate (Q_g) was determined from the actual gas volume, as given in Eq. 8.

$$Q_g = V_g\,/(A_{cat})\,(t) \quad \text{(Eq 8)}$$

where Q_g (L g/m^2 cathode. day) is the gas production rate, A_{cat} (m^2) is the cathode surface area, and t (day) is the production time.

2.5 Output from the MEC Operation

2.5.1 Chemical Oxygen Demand Removal

The change in COD (ΔCOD) values on the anolyte was determined by COD of feed (COD_{feed}) and effluent ($COD_{effluent}$) after four months of operation, as described by Eq. 9, where:

$$\Delta COD = COD_{feed} - COD_{effluent} \quad \text{(Eq 9)}$$

COD removal (COD_{rem}) denotes the amount of COD consumed during MEC operation and was calculated using Eq. 10.

$$COD_{rem} = (\Delta COD\,/COD_{effluent}) \times 100 \quad \text{(Eq.10)}$$

2.5.2 Surface Analysis

On day 70, after startup under the Cc-, and Co-MEC systems, the electrodes' surfaces were examined for signs of corrosion using a Field Emission Scanning Electron Microscope (FESEM) (Zeiss, Supra 55VP, Germany). The biofilm sample from the cathode's surface was scraped with a blade, and the clean metal surface was rinsed with ultrapure water and absolute ethanol, then sonicated for 8 hours. Subsequently, the metals were later rinsed with sterile deionised water. A thin Au film was deposited on the electrode surface to enhance electrical conductivity. In addition, the 3D surface roughness of the SS surface before and after the BES operation was characterised using atomic force microscopy (AFM). SS systems were selected because of their superior performance relative to CS. The surface morphology of the SS surface was characterised using a 10 µm × 10 µm AFM scan, to obtain the arithmetical mean height (S_q) and the root mean square height (S_q), both reported in nm.

2.5.3 DNA Extraction and PCR Amplification

A further microbial identification test was conducted using biofilm samples from the SS cathodes of Co-MEC and Cc-MEC systems. The biofilm sample from the SS surface was scraped with a sterile surgical blade for microbial community analysis. SS systems were selected because of their superior corrosion resistance relative to CS. The Wizard® Genomic DNA Purification Kit was used to extract DNA according to the manufacturer's instructions. The DNA pellet was then dehydrated by adding rehydration solution overnight at 4 °C. The DNA concentration was measured using a NanoDrop spectrophotometer. Before use, the DNA samples were stored at - 20 °C. The V4 region of the 16S rRNA gene was amplified using the forward primer 515F and the reverse primer 806R. After PCR, DNA fragments were converted from jagged to blunt ends using T4 DNA polymerase, Klenow Fragment, and T4 Polynucleotide Kinase. 'A' base was added to each 3′ end, and short fragments were removed using Ampure beads to ensure only the qualified library was used for sequencing. The bioinformatics analysis was conducted using the sequence data.

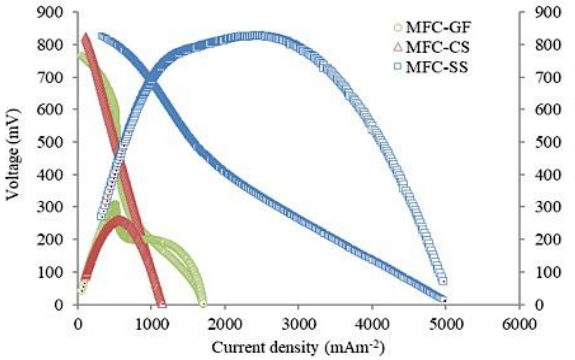

Fig. 3 Power density and polarisation curves of annealed graphite felt, stainless steel and carbon steel anodes in a microbial fuel cell at 70 days of operation

2.5.3.1 Bioinformatics Analysis and Classification of the Microbial Communities

The raw data were filtered to remove adapter pollution, ensuring high-quality sequences. Paired-end reads with overlap, generated using the Illumina HiSeq2500 PE250 platform (Beijing Genomics Institute, Wuhan, China), were merged into tags with an average length of 252 bp and clustered into operational taxonomic units (OTUs) at 97% sequence similarity using scripts from USEARCH v7.0.1090 software. Taxonomic ranks were assigned to the representative sequences of the OTUs using the Ribosomal Database Project (RDP) trained on the Greengenes database with Naïve Bayesian Classifier v.2.2. The OTUs were further clustered using the MOTHUR program (http://www.Mothur.org/wiki/Main-Page). Alpha-diversity analysis included the Chao, ACE, Shannon, and Simpson indices. The abundances at the phylum, class, and genus levels were displayed using bar graphs.

2.5.4 Statistical Analysis

Statistical analysis was conducted to assess the significance of the performance differences among the system types, materials, and operations. Data were analysed using statistical methods, and the mean was calculated from triplicate experiments, with the standard error of the mean. The abundance-based coverage estimator (ACE), Chao1, Shannon, and Simpson were used to identify the species diversity and richness for each system, respectively. In addition, Principal Component Analysis (PCA)

was applied to visualise the differences and similarities in the microbial community relationships between the two systems.

3. Results and Discussion

At day 70, during the MFCs operation, the MFC-SS exhibited a maximum power density of approximately three times higher (827.25 ± 12.31 mW/m^2) than the MFC-CS (260.14 ± 22.22 mW/ m^2) and two times higher compared to MFC-GF (307.89 ± 13.82 mW/m^2) (**Fig. 3**). The result demonstrated that the power density of MFC-SS is significantly greater (T-test, $p < 0.05$) than that of the CS and GF anodes. This result aligns with Eyiuche *et al.*'s study, in which SS underwent flame-oxidised treatment, producing more power relative to a traditional carbon-based electrode (Eyiuche *et al.*, 2017). Several key factors that may contribute to the SS results include changes in surface morphology, post-annealing elemental concentrations that enhance conductivity, and the transition of the passive layer (Jadhav *et al.*, 2021; M. Zhang *et al.*, 2019; Y. G. Zhao *et al.*, 2017). For instance, the surface morphology of SS plates before and after annealing at 600 °C clearly shows differences in surface roughness (**Fig. 4**). The S_q was 112.97 nm, and the S_a was 87.41 nm for untreated SS. After heating, obvious grooves or piles formed on the treated SS surface with the increased value of 200.81 nm and 160.45 nm for S_q and S_a, respectively, which favours in biofilm formation.

3.1 Performances of MECs With Different Cathode Materials

The amount of hydrogen gas produced (Q_{H_2}) is a typical indicator of the MEC's cathode performance. Table 1 compares the performance of MECs with different cathode materials reported in other studies. The results showed that the modified CC and SS materials yielded higher Q_{H2} (>70 LH_2/m^2.day) with the addition of conductive substances, including PANI, graphene, and Platinum-Group Metals (PGM). These costly conductive substances can lower the HER overpotential, as exemplified by the NiF material, which is 10 times more expensive than SS per 1 cm^2 . In this study, materials were used without costly modification. The plain Cc-MEC-SS gave the highest Q_{H_2} (2.33 ± 0.34 LH_2/m^2.day), 1.3% higher than GF and 54% higher than Cc-MEC-CS, and slightly higher than the Q_{H_2} performance of SSM modified with PANI and graphene (Huang *et al.*, 2011) and SSB, which has a high surface area (Call *et al.*, 2009). In addition to hydrogen production, the MEC produced a small amount of methane, accounting for up to 30% of the total Q_{H_2} and Q_{CH_4}.

Hydrogen production is associated with a reduction in COD, as organic matter in the anolyte is consumed. The microorganism oxidised organic substances to simpler molecules, such as lactate and butyrate, thereby reducing COD, and hydrogen was produced as a by-product. In Table 1, only Q_{H_2} from the SS cathode modified with conductive substance showed a comparable COD reduction performance (Ghasemi *et al.*, 2020). The unmodified NiF electrode (Guerrero-Sodric *et al.*, 2024), although Q_{H_2} is 10 times higher than Cc-MEC-CS, Cc-MEC-GF and Cc-MEC-CS in this study, COD removal is within the same range (~40%). The COD removals and recorded Q_{H_2} trends align with the I_v, with MECs with SS (1.08 A/m^2) higher than the GF (by 17%) and CS (by 23%). While energy production plays a crucial role in BES for selecting or developing EAB (Choi & Sang, 2016), corrosion behaviour of the materials becomes a relevant factor when evaluating the performance of metal electrodes. This highlights the need to consider corrosion resistance when selecting materials for MEC biocathodes while maintaining hydrogen production.

The selection of cathode materials significantly influences the performance of MECs in producing valuable chemicals or biogas (Bora *et al.*, 2022; Huang *et al.*, 2011; Swaminathan *et al.*, 2024). Carbon materials are commonly used as cathodes in MECs owing to their high catalytic stability and efficiency. However, research on other materials, such as Ni, SS, and GF, is ongoing to improve MEC efficiency (K. Y. Kim & Logan, 2019; Rossi *et al.*, 2023; Yun *et al.*, 2021). SS is an attractive alternative to carbon materials because it reduces polarisation resistance, bacterial affinity, and mechanical fragility, and improves durability. However, the smooth surface of SS can pose a challenge for microbial attachment, often necessitating surface modifications (Kundu *et al.*, 2013; Rivera *et al.*, 2017). Kundu *et*

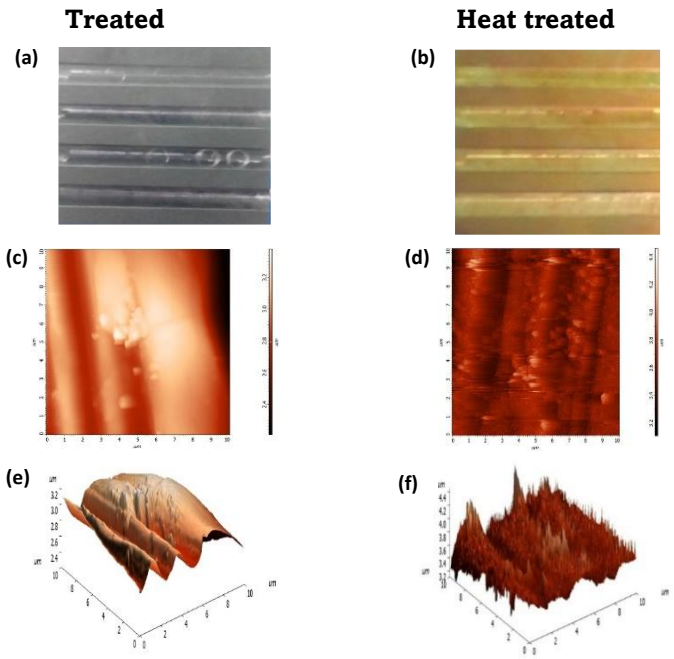

Fig. 4 Surface morphology of SS plates before and after annealing at 600 °C for 5 minutes; (a, b) Untreated and heat-treated SS plates, (c, d) AFM micrograph 2D of untreated and heat-treated SS, and (e,f) 3D micrograph of untreated and heat-treated SS at 10 µm × 10 µm AFM scan

Table 1
Performance of MECs with different cathode materials

Cathodes	Catalysts	COD removal (COD_{rem}) %	Current generated (I_v) A	Q_{H2} = Hydrogen production rate LH_2/ m^2.day	Q_{CH4} = Methane production rate LCH_4/ m^2.day	References
SSB	Biocathode	-	-	1.42 ± 0.20	-	(Call *et al*., 2009)
SSM	Biocathode	-	0.006	2100 ± 0.30 LH_2/ m^3.day	-	(Y. Zhang *et al*., 2010)
SSM	PANI, graphene	82	-	805 LH_2/ m^3.day	-	(Ghasemi *et al*., 2020)
HSSF	Biocathode	-	-	-	1.0	(Liu *et al*., 2017)
CC	Pd nanoparticle	-	-	2.60 ± 0.50	-	(Huang *et al*., 2011)
CC	Pt carbon	-	-	73.6 ± 0.0022	-	(Rozenfeld *et al*., 2019)
GF	Biocathode	-	-	-	1.0	(Liu *et al*., 2017)
GAC	Biocathode	-	35.0	-	65.0	(Liu *et al*., 2018)
NiF	Biocathode	40.0	2.00	19.07 ± 0.46	-	(Guerrero-Sodric *et al*., 2024)
Results in this study:						
SS	Biocathode	45.0	1.08	2.33 ± 0.34 466 ± 0.34 LH_2/ m^3.day	0.53 ± 0.01	(This study)
GF	Biocathode	44.0	0.90	2.30 ± 0.01 460 ± 0.34 LH_2/ m^3.day	0.54 ± 0.01	(This study)
CS	Biocathode	38.0	0.83	1.07 ± 0.05 214 ± 0.34 LH_2/ m^3.day	0.44 ± 0.01	(This study)

SS = stainless steel; CS = carbon steel; GF = graphite felt; HSSF = heat-treated stainless steel felt; NiF = Nickel foam; SSM = stainless steel mesh; SSB = stainless steel brush; GAC = granular activated carbon; Pd = palladium; CC = carbon cloth

al. reported that SS's QH2 was 2.2 times higher than the Pt sheet metal (Kundu *et al*., 2013). This study used annealed GF, SS, and CS as cathodes in an MEC system with bioanodes enriched from MFCs (Shamsuddin *et al*., 2018). The findings showed that MEC systems with SS achieved the highest COD removal rate and Q_{H2} production rate, followed by GF and CS.

Theoretically, higher COD will reflect higher Q_{H2}, however, there are other contributing factors like applied voltage, electrode material, microbial community and integration of the MEC system that can be considered for performance improvement. Consequently, SS annealing can promote biofilm formation, which is necessary for MEC performance, without requiring expensive catalysts such as PGM or PANI. During an MEC operation, electrons flow from the anode to the cathode. Illes *et al*. noted that electrochemical corrosion could occur when electrons from atoms on the metal surface freely flow into the electrolyte (Illés *et al*., 2015). Meanwhile, the EAB at the cathode accepts electrons from the cathode to facilitate further reduction reactions (Shamsuddin *et al*., 2019; Y. C. Zhang *et al*., 2015). Hence, it is crucial to select or develop the EAB at the cathode and to evaluate the corrosion resistance of metal electrodes.

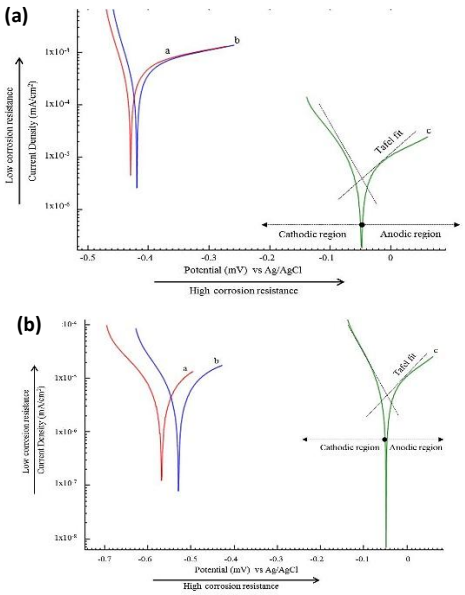

Fig. 5 Polarisation curves in the (a) open-circuit and (b) closed-circuit systems 1 mV/s scan rate, with an application of: carbon steel, a; stainless steel, b, and graphite felt, c, cathode, after immersion in biotic culture media for up to 120 days

3.2 Corrosion Resistance Analysis

Some Cc-MEC systems were subsequently operated under open-circuit conditions after hydrogen was collected under closed-circuit conditions. The corrosion current density, I_{corr}, is determined from the Tafel plot by extrapolating the linear portion of the curve to the corrosion potential. Figure 5 shows the PDP curves of the three types of cathode materials in Co-MEC and Cc-MEC systems after immersion in biotic culture media for up to 120 days.

The parameter values were obtained from the Tafel fit provided by the NOVA software. Under the Co-MEC setting, the MEC-SS exhibited an average I_{corr} of approximately 92% lower

Table 2
Experimental potentiodynamic polarisation parameters for open and closed-circuit systems biocathodes (Ag/AgCl as the reference electrode, at 120 days of operation and scan rate of 1 mV/s)

	I_{corr} (μA/cm^2)	R_M (mm/year)
Closed-circuit (Cc)		
SS	2.91 ± 2.53	0.03 ± 0.03
CS	6.97 ± 7.59	0.08 ± 0.08
GF	2.81 ± 2.73	0.03 ± 0.03
Open-circuit (Cc)		
SS	3.81 ± 1.96	0.04 ± 0.03
CS	50.51 ± 53	0.59 ± 0.62
GF	3.16 ± 2.84	0.03 ± 0.03

Table 3
Chemical composition of electrodes annealed at 600 °C based on EDX analysis in this study

Electrodes	Composition (wt%)					
	Fe	O	C	Cr	Mo	N
SS	37.6	9.1	2.1	36.1	6.2	0.0
CS	67.9	27.4	3.1	0.0	0.1	0.5
GF	0.0	5.2	93.0	0.0	1.6	0.0

than the MEC-CS cathode and 21% higher than MEC-GF (3.16 ± 2.84 μA/cm^2) (Table 2). A similar trend was observed in the Cc-MEC setting, where the MEC-SS exhibited an average I_{corr} approximately 58% lower than that of the MEC-CS cathode, whereas it was 4% higher than that of the MEC-GF (2.81 ± 2.73 μA/cm^2).

I_{corr} is a key component in determining R_M (Eq.6), with higher I_{corr} values indicating faster corrosion (Eq.6). SS's R_M in Co-MEC conditions was 93% lower than CS (0.59 mm/year) and 33% higher than GF (0.03 mm/year). Meanwhile, under Cc-MEC conditions, the SS was 63% lower than the CS (0.08 mm/year) and had an R_M similar to that of the GF (0.03 mm/year). The Cc-MEC showed that the R_M of the electrode materials could be lowered, especially when using CS as electrodes.

The biofilm plays a role in the MIC (Lou *et al*., 2021; E. Zhou *et al*., 2022). When a metal is submerged in an electrolyte, electrochemical reactions occur at the metal/solution interface, creating an electrochemical condition known as an open-circuit potential (Jia *et al*., 2019; Lou *et al*., 2021). In the developed Co-MEC system, the corrosion of SS and CS was primarily influenced by the inherent metal properties (e.g., standard potentials and alloy composition), material surface imperfections, and biological conditions (including biofilm formation and microbial metabolic by-products).

Compared to the SS, CS has a higher iron concentration and a much lower chromium concentration (TWI Ltd, 2024) (Table 3), which may be why the I_{corr} is higher in CS once corrosion is evident. These results provide initial evidence of SS's corrosion resistance, as it exhibits greater anodic dissolution resistance and slower degradation rates. The I_{corr} values were obtained from the curves according to the standard approach. GF, serving as the control, demonstrated the lowest I_{corr} and R_M values, indicating excellent corrosion resistance. Based on the data presented in Table 2, SS demonstrates favourable electrochemical performance as a cathode material under both Cc-MEC and Co-MEC conditions. Compared with CS, SS exhibits superior corrosion resistance. CS showed significantly higher I_{corr}, particularly under Co-MEC conditions, leading to a higher R_M of 1.02 ± 0.62 mm/year. The elevated I_{corr} and R_M values for CS indicate a greater susceptibility to corrosion, making it less suitable for long-term applications in similar environments. The low I_{corr} reported by SS may be due to chromium concentrations generally above 10.5%, which form a passive oxide layer on the SS surface, thereby making it corrosion-resistant. While GF exhibits superior corrosion resistance, SS offers adequate corrosion resistance, mechanical robustness, and electrical properties, positioning it as a suitable cathode material for various electrochemical applications (Abu Bakar *et al*., 2018; Gao *et al*., 2024; Kundu *et al*., 2013; Liu *et al*., 2017).

In addition, Figure 6shows the FESEM images of the SS and CS cathodes from Co-MEC and Cc-MEC systems after 70 days of operation. Fig 6 (a) shows that approximately 5 to 30 μm wide pitting corrosion was observed on the Co-MEC-SS cathode, while no pits were seen in Cc-MEC-SS. Similarly, a small 10 μm pit was observed in Cc-MEC CS. In contrast, Co-MEC-CS displayed several large holes with diameters of up to 50 μm (Fig 6b). Consequently, the CS cathode experienced more corrosion in Co-MEC than in Cc-MEC, with approximately three pits compared to one per SEM view. According to FESEM images, the cathodes most impacted by corrosion were SS and CS, with SS exhibiting a pit width roughly 1.5 times smaller than that of CS. Additionally, SRB sulphide production frequently results in the formation of pits on SS and CS surfaces. The corrosion-causing sulphide is converted to hydrogen sulphide, which subsequently reacts with iron to form an iron sulphide layer. Particularly in a closed system, the iron sulphide layer can become unstable, leading to pitting and localised corrosion (Pessu *et al*., 2021). The iron sulphide concentration increases with the metal's corrosion rate (Guan *et al*., 2016). *Desulfovibrio* bacteria, which were detected as the dominant genus in this study, are generally known for their ability to cause destructive metal corrosion (Beese-Vasbender *et al*., 2015; Guan *et al*., 2016). Some studies have reported that these microorganisms can induce metal corrosion by directly accepting electrons (Coetser & Cloete, 2005; Kato, 2016; Lou *et al*., 2021). Additionally, research by Li *et al*. revealed pit corrosion caused

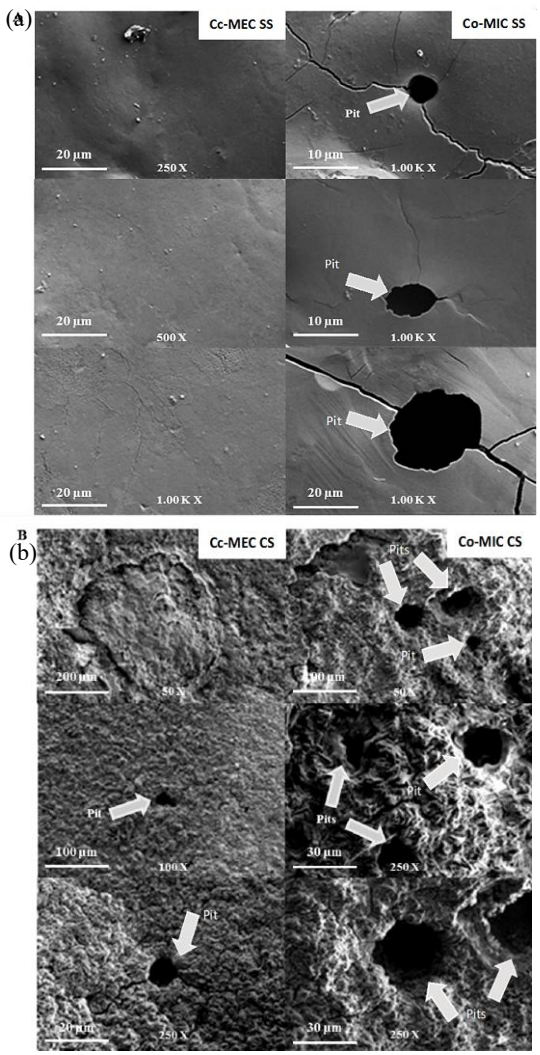

Fig. 6 The surface morphology of (a) stainless steel and (b) carbon steel cathodes in open (right) and closed (left) circuit Co-MEC and Cc-MEC systems after 70 days of operation at various magnifications (50 X, 100 X, 250 X, 500 X and 1 kX)

Table 4
Alpha diversity analysis

Systems	ACE	Chao1	Shannon	Simpson
Cc-MEC	731.79	727.68	3.84	0.05
Co-MEC	692.69	685.88	4.04	0.05

by *D. vulgaris* in the presence of an electron mediator on metal (H. Li *et al*., 2015).

3.4 Microbial Richness and Diversity

This study investigated the bacterial communities on SS cathode samples of Cc-MEC and Co-MEC. Amplicon sequencing, using the Illumina HiSeq 2500 platform with a paired-end (PE) 250-bp read length, was employed to identify the bacteria present. A total of 707,358 tags with 353,679 high-quality reads and an average length of 252 bp were obtained. The analysis revealed a higher number of unique operational taxonomic units (OTUs) in the Cc-MEC samples than in the Co-MEC samples (723 vs. 676 OTUs). This suggests a greater richness of bacterial life in the Cc-MEC environment. Further analysis using diversity indices (ACE, Chao1, Shannon, and Simpson) confirmed this trend. The ACE and Chao1 values for Cc-MEC were higher than those for Co-MEC, with an average of 729.73 and 689.28, respectively (Table 4). The Cc-MEC samples exhibited higher richness values (ACE and Chao1), indicating a more significant number of bacterial species (average of 729.73). Conversely, the Co-MEC samples displayed higher Shannon and Simpson values (average of 2.04), suggesting greater diversity within the fewer bacterial species.

As mentioned earlier, biofilms can significantly alter the physicochemical properties of metal surfaces, accelerating metal deterioration. However, biofilms can also enhance current and power production in BES. In BES, EAB can transfer electrons between their cells and the electrode (G. W. Chen *et al*., 2010; Choi & Sang, 2016). Bacterial metabolism at the anode (Choi & Sang, 2016; E. Zhou *et al*., 2022) releases electrons from the oxidation of organic matter, which are transported to the anode surface and then flow to the cathode. Interestingly, the continuous supply of electrons from the EAB at the anode to the cathode via an external circuit may function like CP. Using sacrificial anodes or impressed current as part of CP has significantly reduced metal surface corrosion rates (Shamsuddin *et al*., 2019; Wang *et al*., 2020). Some studies suggest that the continuous electron supply from an enriched anodic biofilm can function similarly to an impressed current in CP, thereby preventing metal corrosion (Orfei *et al*., 2006; Y. C. Zhang *et al*., 2015; E. Zhou *et al*., 2022). Xu *et al*. also argued that certain microbial activities enhance metal corrosion resistance, potentially offering a novel CP technique (F. L. Xu *et al*., 2015). Under free-oxygen conditions, this study observed substantially lower annual pit or corrosion loss for SS and CS cathodes in Cc-MEC than in Co-MEC. This effect demonstrates that MECs can exhibit CP, which benefits cathode metals, particularly CS, which experiences much less corrosion than under open-circuit conditions. The biofilm at the MEC anode supplies electrons to protect the cathode, while the microbes involved in metal corrosion use these electrons instead of oxidising the metal cathode (Orfei *et al*., 2006; Suhaili & Samsudin, 2018).

3.5 Microbial Community Analyses from SS cathode of Co-MEC and Cc-MEC systems

The nine most abundant taxa at the phylum level were abridged in Fig 7a, while the non-assigned OTUs (approximately 37.0%) were removed. Hence, the total percentage did not reach 100%, with most OTUs clustered within three phyla for both samples. Proteobacteria were the most abundant phylum, with a relative abundance of up to 45.49% in Cc-MEC. Consistent with prior research (Croese *et al*., 2011), the relative abundance of Proteobacteria in Co-MEC was up to 30.92%, with Bacteroidetes as the second most abundant phylum at an average of 22.67%. Bacteroidetes have been reported to enrich cathodes in MEC (Xafenias & Mapelli, 2014). Firmicutes exhibited a similar high diversity in both systems, ranging from 7.50% to 7.60%. Other minor phyla included Actinobacteria, Chloroflexi, Fusobacteria, Spirochaetes, and Synergistetes, with average relative abundances of 1.34%, 0.01%, 0.14%, and 0.47%, respectively. The phyla present in Cc-MEC and Co-MEC samples were nearly identical, except for Chlamydiae, which was observed in the Co-MEC system at a relative abundance of less than 0.01%.

Nine classes were identified in both Cc-MEC and Co-MEC samples, as shown in Fig 7b. Deltaproteobacteria exhibited high relative abundances of up to 23.02% and 25.54% in Cc-MEC and Co-MEC, respectively. Beta-, Gamma-, and

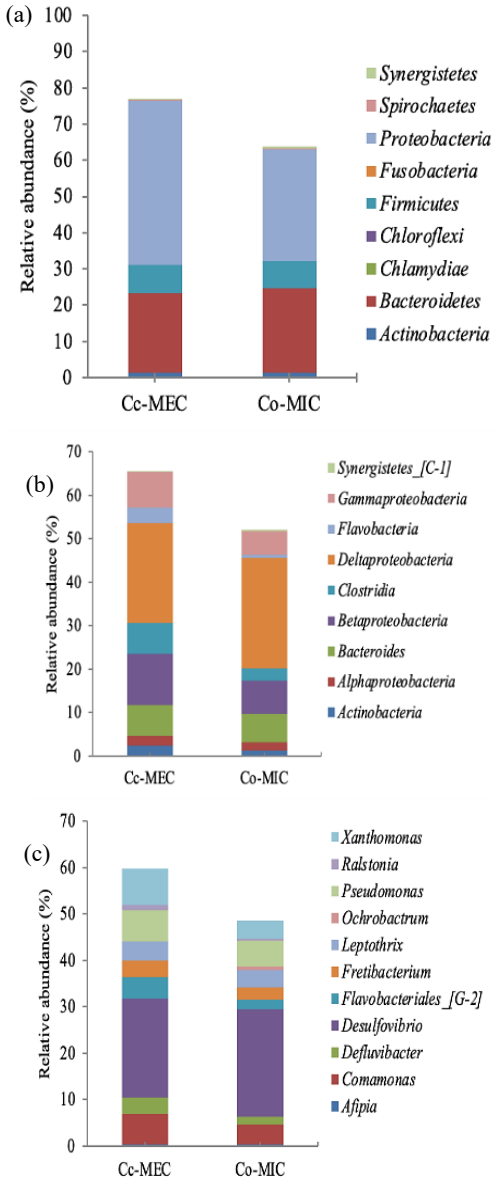

Fig 7. Relative abundances of bacterial 16S rRNA gene sequences from closed-circuit and open circuit presented at the: (a) phylum level, (b) class level, and (c) genus level

Alphaproteobacteria were also detected, with relative abundances ranging from 1.94% to 11.74% in Cc-MEC and 5.33% to 7.58% in Co-MEC. Deltaproteobacteria are commonly dominant in biocathodes and biocorrosion studies, while the Proteobacteria phylum subclass plays a crucial role in the hydrogen evolution reaction in MEC biocathodes (G. W. Chen *et al*., 2010; Croese *et al*., 2011; Dykstra & Pavlostathis, 2017; B. H. Kim *et al*., 2015; H. Li *et al*., 2015; Y. C. Zhang *et al*., 2015). Clostridia and Actinobacteria (ranging from 1.25% to 7.14%), detected in this study, have been identified in other research on the MEC biocathode (Croese *et al*., 2011; Dykstra & Pavlostathis, 2017) and corroded metal (X. Li *et al*., 2017). However, Flavobacteria and Synergistetes exhibited lower sequencing depth under Co-MEC (0.62%) than under Cc-MEC (1.90%).

Figure 7(c) depicts the relative abundance of Cc-MEC and Co-MEC samples at the genus level to compare the microbial communities of the two systems. *Desulfovibrio* was the dominant genus shared by both samples, which thrives between pH 4.0 and 9.5, while actives cause corrosion between pH 6.5 and 7.0 (Fan *et al*., 2023; X. Li *et al*., 2017). About 21.31% and 23.21% of the Deltaproteobacteria identified in Cc-MEC and Co-MEC's class levels belonged to the *Desulfovibrio*. The class Betaproteobacteria was composed primarily of the genera *Comamonas, Leptothrix*, and *Ralstonia,* with average abundances of 3.90% and 2.82% in Cc-MEC and Co-MEC, respectively. They commonly thrive between pH 6.0 and 7.5 (Eggerichs *et al*., 2014; St Clair *et al*., 2019). The class of Gammaproteobacteria from the genera of *Pseudomonas* and *Xanthomonas*, which commonly thrive at pH between 6.0 and 7.7 (Cho *et al*., 2016), showed a higher abundance (average 7.31%) in Cc-MEC than in Co-MEC (average 4.79%). The numbers of Alphaproteobacteria and Synergistia, including the genera *Defluvibacter, Afipia, Ochrobactrum,* and *Fretibacterium*, were similar in both samples (ranging from 0.13 to 3.51%). Meanwhile, Flavobacteria thrive at pH levels ranging from 6.0 to 8.5, with optimal growth occurring around neutral pH levels (Jin & Jeon, 2015; Patil *et al*., 2018). They were detected in Cc-MEC with a relative abundance of 4.71%, compared to 2.04% in Co-MEC.

This study demonstrates that bacteria from various genera, including *Desulfovibrio, Comamonas, Leptothrix, Ralstonia, Pseudomonas*, and *Xanthomonas*, grow within a typical pH range of 6.0 to 7.7 for both systems. *Desulfovibrio* sp., a genus within the SRB group, was the highest quantity in both systems. The SRB group of bacteria is commonly known to change sulphate to sulphide, mainly hydrogen sulphide, which is a corrosive agent (Eq. 11) (Guan *et al*., 2016; Jia *et al*., 2019). During SRB corrosion, a biofilm layer comprising SRB cells, water, extracellular polymeric substances (EPS), and corrosion products forms on the metal surface, influencing metal dissolution (Akpoborie *et al*., 2021; J. Chen *et al*., 2019). Microbes can contribute to corrosion both directly and indirectly. Direct corrosion occurs when the SRBs induce metal corrosion through enzymatic or EPS reactions, facilitating electron flow and cathodic hydrogen consumption (Fan *et al*., 2023; Kato, 2016). The cathodic hydrogen formed on the metal surface can promote the growth of SRBs.

$$SO_4^{2-} + 4H_2 \rightarrow S^{2-} + 4H_2O \quad \text{(Eq. 11)}$$

Meanwhile, indirect corrosion occurs via chemical attack, in which the SRB biofilm, containing iron sulphide, accelerates metal corrosion by releasing hydrogen sulphide. This reaction depletes protective chromium oxides, thereby creating localised corrosion, such as pits and crevice corrosion. Besides the SRB bacteria, the genus *Pseudomonas*, which is abundant in Cc-MEC, is also involved in biocorrosion; however, to a minor degree than the SRB (Chugh *et al*., 2022; L. Xu *et al*., 2023). The presence of MIC bacteria in this study is unavoidable, as the inoculum originated from the lake. SS continuous operation on both Cc-MEC and Co-MEC systems showed that within 70 days of operation, the Cc-MEC-SS had no corrosion pits (Fig 6(a)). This observation aligns with the taxonomic findings (Fig 6(c)), in which the Cc-MEC system exhibited a higher relative abundance of genera associated with EAB, such as *Comamonas (+3.5%)* and *Pseudomonas (+2%),* compared to the Co-MEC system. These EAB are proposed to contribute to corrosion mitigation by interfering with SRB growth primarily through competitive exclusion, efficient electron utilisation, and biofilm dynamics. *Pseudomonas* species, for instance, are involved in biocorrosion and also inhibit SRB through EPS production and biofilm formation, which can lead to reduced localised corrosion, for instance, the corrosion behaviour of CS in the presence of *Escherichia coli* and *Pseudomonas fluorescens* biofilm in reclaimed water (Maji & Lavanya, 2024; Sun *et al*., 2022; P. Xu *et al*., 2020). Mechanistically, under closed-circuit conditions, the cathode with a heat-treated surface likely facilitated a more robust 'microbe-to-metal' interface. The quantitative abundance of these genera supports the conclusion that the annealed SS surface lowered the activation overpotential by increasing the number of active biological sites per geometric cm^2. Simultaneously, these genera degrade organic matter, thereby indirectly facilitating hydrogen production (Eq. 2).

4. Conclusion

This study assesses the effectiveness of an MEC system in preventing microbial corrosion of metals such as SS and CS. The focus is on key MEC-related factors, such as hydrogen gas production and COD removal, while also providing evidence of corrosion. Therefore, a meticulous investigation was conducted on the performance of SS biocathodes compared to CS and GF (control) electrodes under both closed-circuit and open-circuit conditions. The findings, while promising for hydrogen production, highlight SS's vulnerability to corrosion and emphasise the need for strategies to mitigate it. The study demonstrated that in a closed-circuit system, SS biocathodes exhibited the highest hydrogen yield, exceeding those of the control GF and CS systems. This superior performance can be attributed to SS's inherent properties, making it a suitable material for biocathode applications. However, the electrochemical analysis revealed a higher susceptibility of CS to corrosion than SS, particularly under open-circuit conditions. This observation was further confirmed by pits on the CS surface, indicating the corrosive effects of the microbial environment. Microbial community analysis provided crucial insights into the fundamental corrosion mechanisms and potential mitigation strategies. Under open-circuit conditions, a higher abundance of the class Deltaproteobacteria, known for their metal-reducing properties, was observed on the SS biocathodes. This finding suggests that MIC risk may occur in the absence of an external circuit. Conversely, closed-circuit operation increased Gammaproteobacteria, a class that encompasses numerous EABs. EAB provides CP by altering the electrochemical environment and inhibiting the growth of corrosive microorganisms. The study shows that the SS, compared with the CS and GF, has the potential to be cost-effective as an electrode in MECs, thereby enhancing its prospects for large-scale applications, particularly in wastewater treatment systems. Meanwhile, this result necessitates further research to optimise microbial community composition and operational parameters to mitigate long-term corrosion.

Acknowledgments

The authors thank the Research University Grant Scheme (GUP): GUP-2023-039 and GUP-2015-036, Fundamental Research Grant Scheme (FRGS) (FRGS/1/2014/TK06/UKM/03/1), and the Ministry of Higher Education Malaysia through the Higher Institution Center of Excellence Program to Fuel Cell Institute: Universiti Kebangsaan Malaysia (HICOE-2023-003) in supporting our project under SDG 7. In addition, the authors would also like to thank the staff and technicians of the Fuel Cell Institute for their assistance throughout the project.

Author Contributions: R.A.S.: Methodology, formal analysis, writing—original draft, M.H.A.B.: Supervision, conceptualisation, methodology, writing—review and editing, resources, project administration, validation, W.R.W.D: Supervision, project administration, K.B.H.: Supervision, conceptualisation, methodology, J.M.J: Supervision, W.S.A.W.M.N.: Supervision, R.M.Y.: Supervision, I.S.: Resources, F.N.:Resources. All authors have read and agreed to the published version of the manuscript.

Funding: This research was funded by the Research University Grant Scheme (GUP) (GUP-2023-039). This study is also supported by the Ministry of Higher Education Malaysia through the Higher Institution Center of Excellence Program to Fuel Cell Institute: Universiti Kebangsaan Malaysia (HICOE-2023-003), Fundamental Research Grant Scheme (FRGS) (FRGS/1/2014/TK06/UKM/03/1) and the Research University Grant Scheme (GUP) (GUP-2015-036).

Conflicts of Interest: The authors declare no conflict of interest.

References

Abu Bakar, M. H., Shamsuddin, R. A., Yunus, R. M., Wan Daud, W. R., Md. Jahim, J., & Aqma, W. S. (2018). Stainless steel application as metal electrode in bioelectrochemical system. *Jurnal Kejuruteraan*, *SI1*(1), 65–75. https://doi.org/10.17576/jkukm-2018-si1(1)-09

Akpoborie, J., Fayomi, O. S. I., Agboola, O., Samuel, O. D., Oreko, B. U., & Ayoola, A. A. (2021). Electrochemical corrosion phenomenon and prospect of materials selection in curtailing the challenges. *IOP Conference Series: Materials Science and Engineering*, *1107*(1), 012072. https://doi.org/10.1088/1757-899x/1107/1/012072

Beese-Vasbender, P. F., Nayak, S., Erbe, A., Stratmann, M., & Mayrhofer, K. J. J. (2015). Electrochemical characterization of direct electron uptake in electrical microbially influenced corrosion of iron by the lithoautotrophic SRB Desulfopila corrodens strain IS4. *Electrochimica Acta*, *167*, 321–329. https://doi.org/10.1016/j.electacta.2015.03.184

Bora, A., Mohanrasu, K., Angelin Swetha, T., Ananthi, V., Sindhu, R., Chi, N. T. L., Pugazhendhi, A., Arun, A., & Mathimani, T. (2022). Microbial electrolysis cell (MEC): Reactor configurations, recent advances and strategies in biohydrogen production. *Fuel*, *328*(June), 125269. https://doi.org/10.1016/j.fuel.2022.125269

Bunsen, H. (2010). 8 - Winemaking equipment maintenance and troubleshooting. In C. E. Butzke (Ed.), *Winemaking Problems Solved* (pp. 199–256). Woodhead Publishing. https://doi.org/10.1533/9781845690188.199

Cabrera, S. E., & Agudelo-Escobar, L. M. (2023). Determination of Electrogenic potential and removal of organic matter from industrial coffee wastewater using a native community in a non-conventional microbial fuel cell. *Processes*, *11*(2), 373. https://doi.org/10.3390/pr11020373

Call, D. F., Merrill, M. D., & Logan, B. E. (2009). High surface area stainless steel brushes as cathodes in microbial electrolysis cells. *Environmental Science and Technology*, *43*(6), 2179–2183. https://doi.org/10.1021/es803074x

Chen, G. W., Choi, S. J., Cha, J. H., Lee, T. H., & Kim, C. W. (2010). Microbial community dynamics and electron transfer of a biocathode in microbial fuel cells. *Korean Journal of Chemical Engineering*, *27*(5), 1513–1520. https://doi.org/10.1007/s11814-010-0231-6

Chen, J., Wu, J., Wang, P., Zhang, D., Chen, S., & Tan, F. (2019). Corrosion of 907 steel influenced by sulfate-reducing bacteria. *Journal of Materials Engineering and Performance*, *28*(3), 1469–1479. https://doi.org/10.1007/s11665-019-03927-1

Choi, O., & Sang, B. I. (2016). Extracellular electron transfer from cathode to microbes: Application for biofuel production. *Biotechnology for Biofuels*, *9*(1), 1-14. https://doi.org/10.1186/s13068-016-0426-0

Cho, S. J., Kim, M. H., & Lee, Y. O. (2016). Effect of pH on soil bacterial diversity. *Journal of Ecology and Environment*, *40*(1), 1-9. https://doi.org/10.1186/s41610-016-0004-1

Chugh, B., Sheetal, Singh, M., Thakur, S., Pani, B., Singh, A. K., & Saji, V. S. (2022). Extracellular electron transfer by Pseudomonas aeruginosa in biocorrosion: A Review. *ACS Biomaterials Science & Engineering*, *8*(3), 1049–1059. https://doi.org/10.1021/acsbiomaterials.1c01645

Coetser, S. E., & Cloete, T. E. (2005). Biofouling and biocorrosion in industrial water systems. *Critical Reviews in Microbiology*, *31*(4), 213–232. https://doi.org/10.1080/10408410500304074

Croese, E., Pereira, M. A., Euverink, G. J. W., Stams, A. J. M., & Geelhoed, J. S. (2011). Analysis of the microbial community of the biocathode of a hydrogen-producing microbial electrolysis cell. *Applied Microbiology and Biotechnology*, *92*(5), 1083–1093. https://doi.org/10.1007/s00253-011-3583-x

Dutt, N. (2022). *Editorial Welcome to International Journal of Energy Resources Applications: A Journal Focussing on the Energy Demand and Applications.* 1–4. https://doi.org/10.56896/ijera.2022.1.1.001

Dykstra, C. M., & Pavlostathis, S. G. (2017). Methanogenic biocathode microbial community development and the role of bacteria. *Environmental Science and Technology*, *51*(9), 5306–5316. https://doi.org/10.1021/acs.est.6b04112

Eggerichs, T., Opel, O., Otte, T., & Rück, W. (2014). Interdependencies between biotic and abiotic ferrous iron oxidation and influence of pH, oxygen and ferric iron deposits. In *Geomicrobiology Journal,* 461-472. https://doi.org/10.1080/01490451.2013.870620

Ewing, T., Ha, P. T., & Beyenal, H. (2017). Evaluation of long-term performance of sediment microbial fuel cells and the role of natural resources. *Applied Energy*, *192*, 490–497. https://doi.org/10.1016/j.apenergy.2016.08.177

Eyiuche, N. J., Asakawa, S., Yamashita, T., Ikeguchi, A., Kitamura, Y., & Yokoyama, H. (2017). Community analysis of biofilms on flame-oxidized stainless steel anodes in microbial fuel cells fed with different substrates. *BMC Microbiology*, *17*(1), 1-8. https://doi.org/10.1186/s12866-017-1053-z

Fan, L., Sun, Y., Wang, D., Zhang, Y., Zhang, M., Zhou, E., Xu, D., & Wang, F. (2023). Microbiologically influenced corrosion of a novel pipeline steel containing Cu and Cr elements in the presence of Desulfovibrio vulgaris Hildenborough. *Corrosion Science*, *223*, 111421. https://doi.org/10.1016/j.corsci.2023.111421

Gao, Q., Lu, Y., Wang, Y., Wu, Y., Zhang, C., & Wang, Y. (2024). Electrochemical study on the corrosion behavior of 316L stainless steel in quaternary nitrate molten salt nanofluids for thermal energy storage applications. *Journal of Energy Storage*, *83,* 1-10. https://doi.org/10.1016/j.est.2024.110491

Ghasemi, B., Yaghmaei, S., Abdi, K., Mardanpour, M. M., & Haddadi, S. A. (2020). Introducing an affordable catalyst for biohydrogen production in microbial electrolysis cells. *Journal of Bioscience and Bioengineering*, *129*(1), 67–76. https://doi.org/10.1016/j.jbiosc.2019.07.001

Guan, F., Zhai, X., Duan, J., Zhang, M., & Hou, B. (2016). Influence of sulfate-reducing bacteria on the corrosion behavior of high strength steel eq70 under cathodic polarization. *PLoS ONE*, *11*(9), 1-22. https://doi.org/10.1371/journal.pone.0162315

Guerrero-Sodric, O., Baeza, J. A., & Guisasola, A. (2024). Enhancing bioelectrochemical hydrogen production from industrial wastewater using Ni-foam cathodes in a microbial electrolysis cell pilot plant. *Water Research*, *256,* 1-10. https://doi.org/10.1016/j.watres.2024.121616

Hemdan, B. A., El-Taweel, G. E., Naha, S., & Goswami, P. (2023). Bacterial community structure of electrogenic biofilm developed on modified graphite anode in microbial fuel cell. *Scientific Reports*, *13*(1), 1-14. https://doi.org/10.1038/s41598-023-27795-x

Huang, Y. X., Liu, X. W., Sun, X. F., Sheng, G. P., Zhang, Y. Y., Yan, G. M., Wang, S. G., Xu, A. W., & Yu, H. Q. (2011). A new cathodic

electrode deposit with palladium nanoparticles for cost-effective hydrogen production in a microbial electrolysis cell. *International Journal of Hydrogen Energy*, *36*(4), 2773–2776. https://doi.org/10.1016/j.ijhydene.2010.11.114

Illés, B., Hurtony, T., & Medgyes, B. (2015). Effect of current load on corrosion induced tin whisker growth from SnAgCu solder alloys. *Corrosion Science*, *99*, 313–319. https://doi.org/10.1016/j.corsci.2015.07.026

Jadhav, D. A., Pandit, S., Sonawane, J. M., Gupta, P. K., Prasad, R., & Chendake, A. D. (2021). Effect of membrane biofouling on the performance of microbial electrochemical cells and mitigation strategies. In *Bioresource Technology Reports* (Vol. 15), 1-15. https://doi.org/10.1016/j.biteb.2021.100822

Jia, R., Unsal, T., Xu, D., Lekbach, Y., & Gu, T. (2019). Microbiologically influenced corrosion and current mitigation strategies: A state of the art review. *International Biodeterioration & Biodegradation*, *137*, 42–58. https://doi.org/10.1016/j.ibiod.2018.11.007

Jin, H. M., & Jeon, C. O. (2015). Litoribaculum gwangyangense gen. Nov., sp. nov., isolated from a sea-tidal flat sediment. *International Journal of Systematic and Evolutionary Microbiology*, *65*(2), 381–387. https://doi.org/10.1099/ijs.0.068684-0

Kato, S. (2016). Microbial extracellular electron transfer and its relevance to iron corrosion. In *Microbial Biotechnology* (Vol. 9, Issue 2, pp. 141–148). John Wiley and Sons Ltd. https://doi.org/10.1111/1751-7915.12340

Khan, M. S., Kakar, F. K., Khan, S., & Athar, S. O. (2018). Efficiency and cost analysis of power sources in impressed current cathodic protection system for corrosion prevention in buried pipelines of Balochistan, Pakistan. *IOP Conference Series: Materials Science and Engineering*, *414*(1), 1-11. https://doi.org/10.1088/1757-899X/414/1/012034

Kim, B. H., Lim, S. S., Daud, W. R. W., Gadd, G. M., & Chang, I. S. (2015). The biocathode of microbial electrochemical systems and microbially-influenced corrosion. *Bioresource Technology*, *190*, 395–401. https://doi.org/10.1016/j.biortech.2015.04.084

Kim, K. Y., & Logan, B. E. (2019). Nickel powder blended activated carbon cathodes for hydrogen production in microbial electrolysis cells. *International Journal of Hydrogen Energy*, *44*(26), 13169–13174. https://doi.org/10.1016/j.ijhydene.2019.04.041

Kundu, A., Sahu, J. N., Redzwan, G., & Hashim, M. A. (2013). An overview of cathode material and catalysts suitable for generating hydrogen in microbial electrolysis cell. In *International Journal of Hydrogen Energy* (Vol. 38, Issue 4, pp. 1745–1757). https://doi.org/10.1016/j.ijhydene.2012.11.031

Li, H., Xu, D., Li, Y., Feng, H., Liu, Z., Li, X., Gu, T., & Yang, K. (2015). Extracellular electron transfer is a bottleneck in the microbiologically influenced corrosion of C1018 Carbon steel by the biofilm of sulfate-reducing bacterium Desulfovibrio vulgaris. *PLoS ONE*, *10*(8), 1-12. https://doi.org/10.1371/journal.pone.0136183

Lim, S. S., Kim, B. H., Da Li, Feng, Y., Wan Daud, W. R., Scott, K., & Yu, E. H. (2018). Effects of applied potential and reactants to hydrogen-producing biocathode in a microbial electrolysis cell. *Frontiers in Chemistry*, *6*(AUG), 1-19. https://doi.org/10.3389/fchem.2018.00318

Liu, D., Roca-Puigros, M., Geppert, F., Caizán-Juanarena, L., Na Ayudthaya, S. P., Buisman, C., & Heijne, A. (2018). Granular carbon-based electrodes as cathodes in methane-producing bioelectrochemical systems. *Frontiers in Bioengineering and Biotechnology*, *9*(JUN), 1-10. https://doi.org/10.3389/fbioe.2018.00078

Liu, D., Zheng, T., Buisman, C., & Heijne, A. (2017). Heat-Treated Stainless Steel Felt as a New Cathode Material in a Methane-Producing Bioelectrochemical System. *ACS Sustainable Chemistry & Engineering*, *5*, 1-8. https://doi.org/10.1021/acssuschemeng.7b02367

Li, X., Duan, J., Xiao, H., Li, Y., Liu, H., Guan, F., & Zhai, X. (2017). Analysis of bacterial community composition of corroded steel immersed in Sanya and Xiamen Seawaters in China via Method of Illumina MiSeq sequencing. *Frontiers in Microbiology*, *8*(SEP), 1-16. https://doi.org/10.3389/fmicb.2017.01737

Long, S., Liu, X., Xiao, J., Ren, D., Liu, Z., Fu, Q., He, D., & Wang, D. (2024). Mitigation of triclocarban inhibition in microbial electrolysis cell-assisted anaerobic digestion. In *Environmental Science & Technology,* 9272-9282. https://doi.org/10.1021/acs.est.3c10604

Lou, Y., Chang, W., Cui, T., Wang, J., Qian, H., Ma, L., Hao, X., & Zhang, D. (2021). Microbiologically influenced corrosion inhibition mechanisms in corrosion protection: A review. *Bioelectrochemistry*, *141*, 107883. https://doi.org/10.1016/j.bioelechem.2021.107883

Maji, K., & Lavanya, M. (2024). Microbiologically influenced corrosion in stainless steel by Pseudomonas aeruginosa: An Overview. *Journal of Bio- and Tribo-Corrosion*, *10*(1), 1-18. https://doi.org/10.1007/s40735-024-00820-w

Maureira, D., Romero, O., Illanes, A., Wilson, L., & Ottone, C. (2023). Industrial bioelectrochemistry for waste valorization: State of the art and challenges. *Biotechnology Advances*, *64*, 108123. https://doi.org/10.1016/j.biotechadv.2023.108123

Mohd Rasid, Z. A., Omar, M. F., & Mohd Nazeri, M. F. (2017). Polarization study of Sn-0.7Cu solder alloy in 1 M hydrochloric solution. *Materials Science Forum*, *888 MSF*, 394–399. https://doi.org/10.4028/www.scientific.net/MSF.888.394

Moura, V., Ribeiro, I., Moriggi, P., Capão, A., Salles, C., Bitati, S., & Procópio, L. (2018). The influence of surface microbial diversity and succession on microbiologically influenced corrosion of steel in a simulated marine environment. *Archives of Microbiology*, *200*(10), 1447–1456. https://doi.org/10.1007/s00203-018-1559-2

Orfei, L. H., Simison, S., & Busalmen, J. P. (2006). Stainless steels can be cathodically protected using energy stored at the marine sediment/seawater interface. *Environmental Science and Technology*, *40*(20), 6473–6478. https://doi.org/10.1021/es060912m

Patil, K. S., Padakandla, S. R., & Chae, J. C. (2018). Flavobacterium amnigenum sp. Nov. isolated from a river. *Journal of Microbiology and Biotechnology*, *28*(9), 1536–1541. https://doi.org/10.4014/jmb.1806.06044

Pessu, F., Barker, R., Chang, F., Chen, T., & Neville, A. (2021). Iron sulphide formation and interaction with corrosion inhibitor in H2S-containing environments. *Journal of Petroleum Science and Engineering*, *207,* 1-13. https://doi.org/10.1016/j.petrol.2021.109152

Rivera, I., Bakonyi, P., & Buitrón, G. (2017). H2 production in membraneless bioelectrochemical cells with optimized architecture: The effect of cathode surface area and electrode distance. *Chemosphere*, *171*, 379–385. https://doi.org/10.1016/j.chemosphere.2016.12.061

Rosenbaum, M., Aulenta, F., Villano, M., & Angenent, L. T. (2011). Cathodes as electron donors for microbial metabolism: Which extracellular electron transfer mechanisms are involved? *Bioresource Technology*, *102*(1), 324–333. http://dx.doi.org/10.1016/j.biortech.2010.07.008

Rossi, R., Nicolas, J., & Logan, B. E. (2023). Using nickel-molybdenum cathode catalysts for efficient hydrogen gas production in microbial electrolysis cells. *Journal of Power Sources*, *560,* 1-9. https://doi.org/10.1016/j.jpowsour.2022.232594

Rozenfeld, S., Hirsch, L. O., Gandu, B., Farber, R., Schechter, A., & Cahan, R. (2019). Improvement of microbial electrolysis cell activity by using anode based on combined plasma-pretreated carbon cloth and stainless steel. *Energies*, *12*(10), 1-15. https://doi.org/10.3390/en12101968

Shaikh, R., Rizvi, A., Quraishi, M., Pandit, S., Mathuriya, A. S., Gupta, P. K., Singh, J., & Prasad, R. (2021). Bioelectricity production using plant-microbial fuel cell: Present state of art. *South African Journal of Botany*, *140*, 393–408. https://doi.org/10.1016/j.sajb.2020.09.025

Shamsuddin, R. A., Abu Bakar, M. H., Wan Daud, W. R., Hong, K. B., & Jahim, J. M. (2019). Can electrochemically active biofilm protect stainless steel used as electrodes in bioelectrochemical systems in a similar way as galvanic corrosion protection? *International Journal of Hydrogen Energy*, *44*(58), 30512–30523. https://doi.org/10.1016/j.ijhydene.2019.03.089

Shamsuddin, R. A., Wan Daud, W. R., Hong, K. B., Jahim, J. M., Abu Bakar, M. H., Aqma Wan Mohd Noor, W. S., & Yunus, R. M. (2018). Electrochemical characterisation of heat-treated metal and non-metal anodes using mud in microbial fuel cell. *Sains Malaysiana*, *47*(12), 3043–3049. https://doi.org/10.17576/jsm-2018-4712-14

Shi, X., Liang, Y., Wen, G., Evlashin, S. A., Fedorov, F. S., Ma, X., Feng, Y., Zheng, J., Wang, Y., Shi, J., Liu, Y., Zhu, W., Guo, P., & Kim, B. H. (2024). Review of cathodic electroactive bacteria: Species, properties, applications and electron transfer mechanisms. *Science of The Total Environment*, *946*, 174332. https://doi.org/10.1016/j.scitotenv.2024.174332

Singh, R. P., Zorrilla, S. E., Vidyarthi, S. K., Cocker, R., & Cronin, K. (2022). Dairy plant design, construction and operation. In P. L. H. McSweeney & J. P. McNamara (Eds.), *Encyclopedia of Dairy Sciences (Third Edition)* (pp. 239–252). Academic Press. https://doi.org/10.1016/B978-0-12-818766-1.00197-5

Song, X., Zhang, G., Zhou, Y., & Li, W. (2023). Behaviors and mechanisms of microbially-induced corrosion in metal-based water supply pipelines: A review. *Science of The Total Environment*, *895*, 165034. https://doi.org/10.1016/j.scitotenv.2023.165034

St Clair, B., Pottenger, J., Debes, R., Hanselmann, K., & Shock, E. (2019). Distinguishing biotic and abiotic iron oxidation at low temperatures. *ACS Earth and Space Chemistry*, *3*(6), 905–921. https://doi.org/10.1021/acsearthspacechem.9b00016

Suhaili, M. Z., & Samsudin, M. D. M. (2018). Utilization of wastewater for corrosion prevention of carbon steel pipe using single chamber microbial fuel cells. *Environment & Ecosystem Science*, *2*(2), 47–52. https://doi.org/10.26480/ees.02.2018.47.52

Sun, Y., ter Heijne, A., Rijnaarts, H., & Chen, W.-S. (2022). The effect of anode potential on electrogenesis, methanogenesis and sulfidogenesis in a simulated sewer condition. *Water Research*, *226,* 1-9. https://doi.org/10.1016/j.watres.2022.119229

Swaminathan, P., Ghosh, A., Sunantha, G., Sivagami, K., Mohanakrishna, G., Aishwarya, S., Shah, S., Sethumadhavan, A., Ranjan, P., & Prajapat, R. (2024). A comprehensive review of microbial electrolysis cells: Integrated for wastewater treatment and hydrogen generation. *Process Safety and Environmental Protection* 190, 458–474). Institution of Chemical Engineers. https://doi.org/10.1016/j.psep.2024.08.032

Tahir, M. F., Chen, H., Guangze, H., & Mehmood, K. (2022). Energy and exergy analysis of wind power plant: A case study of Gharo, Pakistan. *Frontiers in Energy Research*, *10,* 1-12. https://doi.org/10.3389/fenrg.2022.1008989

Telegdi, J., Shaban, A., & Trif, L. (2017). Microbiologically influenced corrosion (MIC). In *Trends in Oil and Gas Corrosion Research and Technologies: Production and Transmission* (pp. 191–214). Elsevier Inc. https://doi.org/10.1016/B978-0-08-101105-8.00008-5

TWI Ltd. (2024, December 26). *What is the Difference Between Carbon Steel and Stainless Steel?* TWI Ltd. https://www.twi-global.com/technical-knowledge/faqs/carbon-steel-vs-stainless-steel#:~:text=Though%20they%20have%20the%20same,of%20steel%20its%20respective%20properties.

Wang, F., Xu, J., Xu, Y., Jiang, L., & Ma, G. (2020). A comparative investigation on cathodic protections of three sacrificial anodes on chloride-contaminated reinforced concrete. *Construction and Building Materials*, *246*. https://doi.org/10.1016/j.conbuildmat.2020.118476

Wu, Y., Zhou, Z., Fu, H., Zhang, P., & Zheng, Y. (2022). Metagenomic analysis of microbial community and gene function of anodic biofilm for nonylphenol removal in microbial fuel cells. *Journal of Cleaner Production*, *374*, 133895. https://doi.org/10.1016/j.jclepro.2022.133895

Xafenias, N., & Mapelli, V. (2014). Performance and bacterial enrichment of bioelectrochemical systems during methane and acetate production. *International Journal of Hydrogen Energy*, *39*(36), 21864–21875. https://doi.org/10.1016/j.ijhydene.2014.05.038

Xu, F. L., Duan, J. Z., Lin, C. G., & Hou, B. R. (2015). Influence of marine aerobic biofilms on corrosion of 316L stainless steel. *Journal of Iron and Steel Research International*, *22*(8), 715–720. https://doi.org/10.1016/S1006-706X(15)30062-5

Xu, L., Ivanova, S. A., & Gu, T. (2023). Mitigation of galvanized steel biocorrosion by Pseudomonas aeruginosa biofilm using a biocide enhanced by trehalase. *Bioelectrochemistry*, *154*, 108508. https://doi.org/10.1016/j.bioelechem.2023.108508

Xu, P., Ou, Y., & Wei, Z. (2020). Corrosion behavior of carbon steel in the presence of escherichia coli and pseudomonas fluorescens biofilm in reclaimed water. In *Advances in Science, Technology and Innovation* (pp. 141–144). https://doi.org/10.1007/978-3-030-13068-8_34

Yun, W. H., Yoon, Y. S., Yoon, H. H., Nguyen, P. K. T., & Hur, J. (2021). Hydrogen production from macroalgae by simultaneous dark fermentation and microbial electrolysis cell with surface-modified stainless steel mesh cathode. *International Journal of Hydrogen Energy*, *46*(79), 39136–39145. https://doi.org/10.1016/j.ijhydene.2021.09.168

Yu, Z., Zia-ul-haq, H. M., Irshad, A. ur R., Tanveer, M., Jameel, K., & Janjua, L. R. (2022). nexuses between crude oil imports, renewable energy, transport services, and technological innovation: A fresh insight from Germany. *Journal of Petroleum Exploration and Production Technology*, *12*(11), 2887–2897. https://doi.org/10.1007/s13202-022-01487-0

Zhang, M., Ma, Z., Zhao, N., Zhang, K., & Song, H. (2019). Increased power generation from cylindrical microbial fuel cell inoculated with P. aeruginosa. *Biosensors and Bioelectronics*, *141,* 1-27. https://doi.org/10.1016/j.bios.2019.111394

Zhang, Y. C., Jiang, Z. H., & Liu, Y. (2015). Application of electrochemically active bacteria as anodic biocatalyst in microbial fuel cells. In *Chinese Journal of Analytical Chemistry* (Vol. 43, Issue 1, pp. 155–163). Chinese Academy of Sciences. https://doi.org/10.1016/S1872-2040(15)60800-3

Zhang, Y., Merrill, M. D., & Logan, B. E. (2010). The use and optimization of stainless steel mesh cathodes in microbial electrolysis cells. *International Journal of Hydrogen Energy*, *35*(21), 12020–12028. https://doi.org/10.1016/j.ijhydene.2010.08.064

Zhao, J., Fang, Y., Scheibe, T. D., Lovley, D. R., & Mahadevan, R. (2010). Modeling and sensitivity analysis of electron capacitance for Geobacter in sedimentary environments. *Journal of Contaminant Hydrology*, *112*(1–4), 30–44. https://doi.org/10.1016/j.jconhyd.2009.10.002

Zhao, Y. G., Zhang, Y., She, Z., Shi, Y., Wang, M., Gao, M., & Guo, L. (2017). Effect of substrate conversion on performance of microbial fuel cells and anodic microbial communities. *Environmental Engineering Science*, *34*(9), 666–674. https://doi.org/10.1089/ees.2016.0604

Zhou, E., Lekbach, Y., Gu, T., & Xu, D. (2022). Bioenergetics and extracellular electron transfer in microbial fuel cells and microbial corrosion. In *Current Opinion in Electrochemistry* (Vol. 31), 1-7. Elsevier B.V. https://doi.org/10.1016/j.coelec.2021.100830

Zhou, H., Chhin, D., Morel, A., Gallant, D., & Mauzeroll, J. (2022). Potentiodynamic polarization curves of AA7075 at high scan rates interpreted using the high field model. *Npj Materials Degradation*, *6*(1), 1-11. https://doi.org/10.1038/s41529-022-00227-3